Properties of limestone self-compacting concrete at fresh and hardened state

Giovanni Muciaccia[a]*, Sara Cattaneo[b], Gianpaolo Rosati[a] and Stefano Cangiano[c]

[a]*Department of Civil and Environmental Engineering, Politecnico di Milano, Milano, Italy;* [b]*Department of Architecture, Built Environment and Construction Engineering, Politecnico di Milano, Milano, Italy;* [c]*CTG, Italcementi Group, Bergamo, Italy*

(*Received 10 January 2014; accepted 25 August 2014*)

1. Introduction

Self-Compacting Concrete (SCC) use is spreading worldwide and it is becoming the regular solution in some special applications. The denser nature of the mortar phase of SCC with respect to Normal Vibrated Concrete (NVC), due to its own characteristics (fine particles, reduced maximum aggregate size, etc.), is well known (Domone, 2007; Zhu & Bartos, 2003). This peculiar property usually results in an increase in the durability of the structural elements in SCC, basically because the reduced porosity (relative both to the number of porous and to the maximus porous size) slackens the diffusion of external agents into the concrete.

Usually, to reduce the porosity and to increase both the durability and the mechanical properties of concrete, ultra-fine particles are employed, as silica-fume (a by-product of iron-silicon production), whose principle effect is to fill the voids between the cement grains and the aggregates conferring a higher density to the concrete.

In recent years, due to raising difficulties in silica-fume supplying and to some logistic issues concerning its use on big job-sites, the use of silica-fume seems not anymore suitable, favouring the use of limestone as a filler, especially in Europe area.

Recently, the Italian market (especially in the Lombardia region) required special concretes to be used for the construction of high-rise buildings. For this reason, the presented investigation is aimed to the production and the characterisation of a series of SCC mixes which employ as fine particles not silica-fume additions, but rather

*Corresponding author. Email: giovanni.muciaccia@polimi.it

limestone filler. This family of SCC is usually referred to as Limestone Self-Compacting Concrete (LSC).

The use of limestone in replacement of silica-fume is also justified by the high cost of the latter on the Italian market. The enhancement in the properties at both fresh and hardened state is a result of a proper grading of the aggregates and of the limestone filler to obtain a denser and more compact paste.

Since the structural requirements for concrete generally vary according to the function of the structural elements, three different mix profiles were identified, with different requirements:

(1) a LSC designed for a 28 days cubic compressive strength $R_{ck} \geq 40$ MPa and for a low permeability, to be used in foundations (hereafter LSC 40 or Mix 40);
(2) a LSC designed for a 28 days cubic compressive strength $R_{ck} \geq 75$ MPa and for a 1 day compressive strength $R_{ck} \geq 40$, to be used in elevation structures (hereafter LSC 75 or Mix 75); and
(3) a LSC designed for a 28 days cubic compressive strength $R_{ck} \geq 90$ MPa, to be eventually used in specific elements where a very high compressive strength is required (hereafter LSC 90 or Mix 90).

In particular, two different mixes for LSC 90 have been designed in order to maintain their segregation resistance during a time period of one and two hours, respectively. Hereafter, they will be named LSC 90-I and LSC 90-II, respectively.

High fire resistance, low shrinkage and low creep are further requirements for Mix 75. These are ordinary requirements for the cores of tall buildings or for prestressed slabs. High resistance allows the concrete to be competitive with steel structures both in the dimensions of the structural elements and in the costs (in recent years, the costs of steel structures dramatically raised).

As a further requirement each of the four mixes was asked to be rapid-hardening.

The fresh state properties were studied with particular reference to the placing time, as these mixes should be used in complex job-sites. The compressive and bond behaviour at hardened state were successively studied to evaluate the consistency of the models adopted in existing design codes when applied to the investigated concrete mixes (as suggested by Desnerck, De Schutter, and Taerwe [2012]).

The study of the mixes was focused both on their fresh state properties and on their compressive and bond behaviour. All the tests were carried out at the Laboratory of Testing Materials of Politecnico di Milano, unless differently specified.

2. Behaviour at fresh state

In this paragraph, the fresh state behaviour of the Mixes 40, 75, 90 is investigated.

The following fresh state properties have been evaluated, according to EFNARC guidelines (EFNARC, 2005):

- slump-flow (SF)/J-ring;
- time flow T_{500};
- V-funnel;
- L-box;
- U-box; and
- sieve segregation resistance test.

To evaluate the trend over time of the fresh state properties, tests have been performed at different time steps: 0 (t_0), 10, 30, 60, 90 and 120 min after the complete mixing. In a few cases, some steps have not been carried out because of a limited quantity of material available.

As for the sieve segregation test, the fresh concrete was sampled with reference to its weight (4.8 kg) and not to its volume (10 l). SF has been evaluated during the J-ring test (as suggested by Cattaneo and Mola [2012]).

The components of Mixes 40, 75, 90 are reported in Table 1. Exact proportioning is not given because the three mixes are patented.

2.1. *Comparison of properties at fresh state*

In Figure 1, the results of the tests for all the mixes are compared.

LSC 90-II shows the most significant reduction in SF values during the first 60′ (almost 7%), although the remaining properties do not basically change during the first 120′. On the contrary, LSC 40 shows a significant SF reduction during the second hour (-26.3% with respect to $t = t_0$, -22.7% with respect to $t = 60'$).

After 90′ all of the mixes show an evident increase in t_{500}, so in the V-funnel for LSC 75. On the contrary, for LSC 40 V-funnel remains almost constant. A similar comparison is not possible for LSC 90, since complete data at any time are not available because of the reduced amount of material.

Table 2 summarises all the properties of the considered mixes at the fresh state. The experimental values are compared with the requirements both of EFNARC (2005) and of UNI 11040 (2003). Results are grouped, for every mix and every property, for class ranges according to EFNARC classes.

A review of the fresh state properties of the mixes is consequently possible. During the time period of two hours (taken as reference), LSC 40 progressively shifts from class SF3 to class SF1 and from class VS1 to class VS2 (t_{500}) while it remains stable in class VF2 (V-funnel).

According to the classification reported in EFNARC (2005) LSC 40 can thus be used:

- within 30 min (from complete mixing) for floors, slabs and slender elements;
- between 60 and 90 min for walls and piles; and
- up to 120 min only after an adequate evaluation according to the relevant application.

LSC 75 maintains its properties constant during a time period of 120 min. In particular, it is classifiable as SF3 (SF), VS2 (t_{500}) and VF2 (V-funnel). Due to its high

Table 1. Mixes components.

	40	75	90
CEM type	II-AL 42.5R	I 52.5R	
Limestone filler (% vol)	8		
Acrylic superplasticiser (% cement volume)	1.2	2.0	
Water/binder ratio	.50	.35	.33

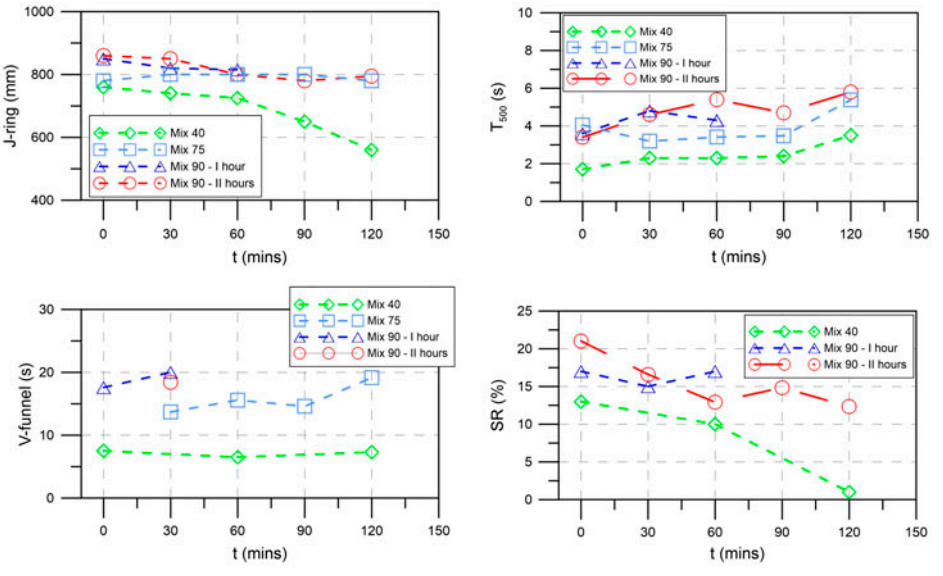

Figure 1. Comparison among fresh state properties of Mixes 40–75–90.

stability, it can be used in all those cases when casting delays can occur. Sieve tests for Mix 75 were not carried out due to the reduced amount of material available at the time of testing.

LSC 90-I keeps its properties constant during a time period of only 60 min, being classifiable as SF3, VS2 (t_{500}) and VF2 (V-funnel), which corresponds to the same classification of LSC 75, even if only during a time period of 60 min.

On the contrary, LSC 90-II is not suitable to be casted during the first 30 min after complete mixing. In fact, according to the Sieve Segregation test, at 10 min its percentage of passing material is under the lower limit allowed by EFNARC guidelines. During this phase, in particular, its SF is greater than 850 mm. For such value, EFNARC guidelines suggest to carefully evaluate segregation issues than can be correlated with high SF values. After 60 min, LSC 90-II can be classified as SF3, VS2 and VF2, as LSC 90-I and LSC 75. However, the higher V-funnel values suggest a careful choice of the job-site machinery for casting.

As drawback, LSC 75 shows a very high viscosity, such that a correct casting on job-site requires the selection of a proper pump.

3. Behaviour at hardened state

The mechanical properties of Mixes 40, 75 and 90 have been deeply investigated, with particular attention drawn on their development over time.

The compressive strength, the elastic secant modulus, the splitting tensile strength and the flexural tensile strength were determined at the laboratories of testing materials of the Universities of Brescia and of Bergamo according to UNI EN 12390-3 (2003), UNI 6556 (1976), UNI EN 12390-6 (2002) and UNI EN 12390-5 (2003), respectively.

The obtained results are summarised in Tables 3 and 4, reporting, for all the mechanical properties, both the mean values and the coefficients of variation (for a

Table 2. Mixes 40, 75, 90 summary of properties at fresh state.

Concrete	Test	*T* (min)	Experimental value	m.u.	EFNARC	UNI
40	*Slump/J-ring*	0	760	mm	SF3	Ok
		30–60	740–725	mm	SF2	Ok
		90–120	650–560	mm	SF1	No (>600 mm)
	t500	0	1.7	s	VS1	Ok
		30–60–90–120	2.3–2.3–2.4–3.5		VS2	Ok
	V-funnel	0–60–120	7.5–6.5–7.3	s	VF1	Ok
	Sieve test	0–60–120	13/10/2001	%	SR2	–
75	*Slump/J-ring*	0–30-60–90–120	780–800–800–800–780	mm	SF3	Ok
	t500	0–30–60–90–120	4.50–3.18–3.41–3.48–5.38	s	VS2	Ok
	V-funnel	30–60–90–120	13.7–15.58–14.6–19.16	s	VS2	No (<12s)
90-I	*Slump/J-ring*	10–30–60	850–820–815	mm	SF3	Ok
	t500	10–30–60	3.4–4.8–4.3	s	VS2	Ok
	V-funnel	ott-30	17.6–20	s	VF2	No (<12s)
	Sieve test	10–30–60	17–15–17	%	SR1	–
90-II	*Slump/J-ring*	10	860	mm	Out of range	Ok
		30–60–90–120	850–800–780–795		SF3	Ok
	t500	10–30–60–90–120	3.4–4.6–5.4–4.7–5.8	s	VS2	Ok
	V-funnel	30	18.4	s	VF2	No (<12s)
	Sieve test	10	21.02	%	Out of range	–
		30	16.6		SR1	–
		60–90–120	12.91–14.85–12.33		SR2	–

number of tested sampler greater than two. Up to three samples were tested for each property).

The compressive and the bond behaviour were successively deeply investigated.

The author focused on the compressive behaviour and on the bond behaviour of each of the different mixes. Bond is considered to be a structural property of concrete, as it will be discussed in paragraph 3.2.

3.1. Compressive behaviour

Tests have been carried out on standard cylindrical specimens (diameter 100 mm, height 200 m) on a MTS servohydraulic closed-loop test machine with a 2500 kN capacity. To follow the post-peak behaviour of all concrete types, different control signals were chosen according to the mechanical properties of the specimens. In particular, higher compressive strength concrete has been expected to be more brittle than ordinary concrete. Therefore, the tests were controlled by the displacement of the actuator (stroke) for LSC40 and by the circumferential strain of the specimen (LSC 75, LSC 90-I and LSC 90-II).

Table 3. Mixes 40, 75, 90 – properties at hardened state, compressive strength and elastic secant modulus – mean value and (CoV).

Concrete	1 day		3 days		7 days		28 days		60 days	
Cubic compressive strength										
40	6.6	(1.8%)	30.5	(3.5%)	37.7	(2.4%)	46.9	(.7%)	50.7	(2.7%)
75	53.4	(1.2%)	79.8	(1.7%)	87.9	(3.7%)	98.6	(1.9%)	102.1	(.7%)
90	62.7	(1.0%)	85.3	–	93.1	(.8%)	104.7	(2.3%)	105.9	(.6%)
Cylindrical compressive strength										
40	6.3	(6.9%)	26.8	(2.4%)	32.3	(4.0%)	42.5	(.9%)		
75	51.0	(2.3%)	70.4	(1.4%)	79.5	(1.9%)	87.9	(1.0%)		
90	65.2	(4.0%)			84.6	(3.3%)	97.3	(1.0%)		
Elastic secant modulus										
40					28176	–	30820	–		
75					42270	–	43520	–		
90					43186	–	46434	–		

Table 4. Mixes 40, 75, 90 – properties at hardened state, tensile strength – mean value and (CoV).

Concrete	1 day		3 days		7 days		28 days		60 days	
Splitting tensile strength										
40	1.6	–	2.3	(4.0%)	2.8	(4.6%)	3.5	(.6%)	3.9	(5.2%)
75	3.4	(4.5%)	4.5	(8.4%)	5.8	(7.4%)	6.3	(11.9%)	6.9	(10.5%)
90	2.2	(25.4%)	4.7	(12.9%)	6.2	(10.4%)	6.6	(5.3%)	7.1	(2.9%)
Flexural tensile strength										
40					4.4	–	5.0	–		
75					6.3	–	7.4	–		
90					6.9	–	7.9	–		

For all the specimens, the vertical displacement has been monitored by three LVDTs on a gauge length of 100 mm, placed at 120°, directly on the lateral surface of the specimen. Additionally, three LVDTs have been placed between the top and bottom platens of the test machine at 120° on a measurement basis of 200 mm. Stearic acid has been spread on both the ends of the specimen to prevent confinement at contact platens.

Table 5 reports the mean and the coefficient of variation (CoV) of both the compressive strength and the strain at the peak for all the mixes. Additionally, the ratio between the average cylindrical and the average cubic compressive strengths is also listed.

The results confirm the value of .85 generally assumed as a ratio between cylindrical and cubic compressive strength for NVC, except for Mix 90 (ratio equal to .93). However, this result agrees with the findings of Klug and Holschemacher (2003) on SCC that reported values of the ratio between the average cylindrical and the average cubic compressive strengths between .9 and 1.

Figure 2 reports, for specimen 40SE28-3, the stress/displacement curves for each of the three transducers directly placed on the specimen. After the peak uniformity is lost as a result of an observable macro-cracking that induces bending effects along the vertical axis of the specimen. As a consequence, the corresponding stress–strain relationship, with the strain evaluated from the displacements recorded by the three transducers on a

Table 5. Compressive strength and deformation properties for Mixes 40, 75, 90.

Code	Compressive strength fcm (MPa)	Average (MPa)	Coef. of variation (%)	Strain at peak (%)	Average (%)	Coef. of variation	fcm/ Rcm
40SE28–1	38.8	38.1	4.5	2.249	2.096	13.0%	.84
40SE28–2	36.2			1.782			
40SE28–3	39.4			2.258			
75SE28–1	85.9	83.7	6.2	2.503	2.335	17.9%	.85
75SE28–2	77.8			1.859			
75SE28–3	87.4			2.642			
90SE28–1	97.7	92.0	7.7	2.710	2.697	.48%	.93
90SE28–2	94.2			2.684			
90SE28–3	84.1			2.698			

measurement basis of 100 mm, is not significant since it presents an unstable behaviour after the peak strain.

As a consequence, the post-peak branch of the compressive stress–strain relationship can only be evaluated from the compressive stress–actuator displacement curve by subtracting the stiffening contribution of the reaction frame. Figure 3 finally reports the compressive stress–strain curves for all the LSC 40 specimens. It can be seen that the softening branch is explored (in relation to the average stress vs. the global average vertical displacement relationship), with a decrease in stiffness around a strain value of 4.0‰, probably due to a change in the structural response of the specimen. Additionally, a non-linear stress–strain relationship for a C30/35 concrete is plotted (Equation (1), according to Eurocode 2 (EC2, 2004)). The two dashed vertical lines indicate a 2.2 and 3.5‰ strain, respectively, corresponding to the strain at peak and to the ultimate strain according to EC2.

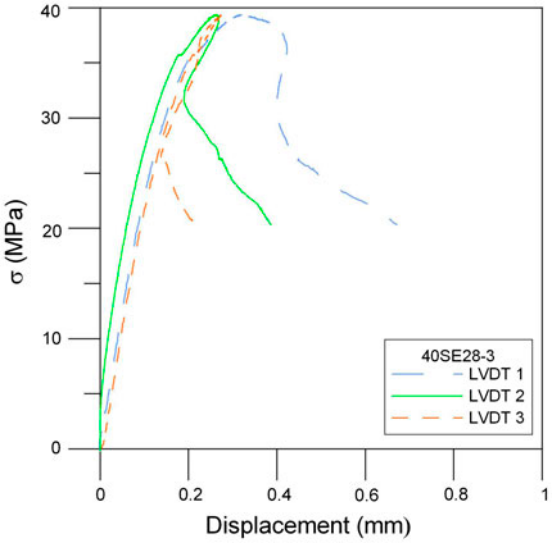

Figure 2. LSC 40 – Compressive stress/displacement curves, measurement basis 100 mm on the specimen.

$$\frac{\sigma_c}{f_{cm}} = \frac{k\eta - \eta^2}{1 + (k-2)\eta} \tag{1}$$

where:

- $\eta = \varepsilon_c/\varepsilon_{c1}$;
- ε_{c1} is the strain at peak stress; and
- $k = 1.05E_{cm} \times |\varepsilon_{c1}|/f_{cm}$.

The post-peak unstable behaviour is much more evident for Mixes 75 and 90. Due to the higher brittleness, the average stress vs. average strain curve can be plotted only up to a point just after the peak. A comparison among all the mixes is reported in Figure 4.

This very high brittleness results in a very unstable behaviour, even when the average circumferential stress is chosen as feedback signal of the servo-controller. This is evident in Figure 5, where the compressive stress is plotted against the vertical displacement for 90SE28-2. The snap-back behaviour before the peak (red circle) suggests that the choice of a different control signal could have resulted in a sudden failure for a lower value of the maximum applied load.

Finally, a comparison between the experimental results and the predictions of EC2 for a NVC of the same concrete class can be carried out for the following properties (see Figure 6):

- compressive strain at the peak stress (ε_{c1});
- ultimate compressive strain (ε_{cu1});
- secant modulus of elasticity (E_{cm}); and
- mean value of flexural tensile strength (f_{ctm}).

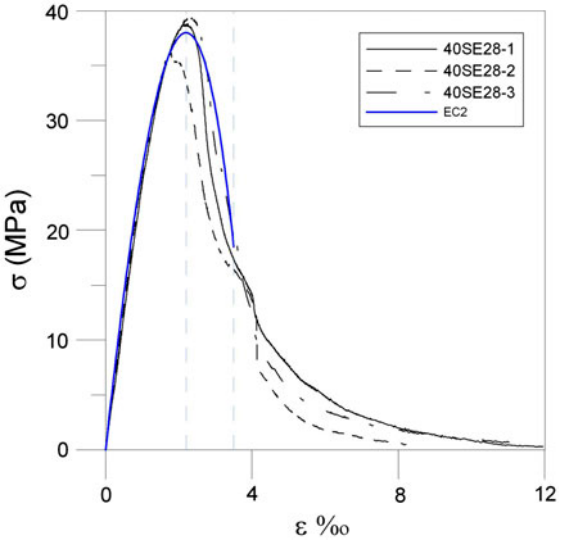

Figure 3. LSC 40 – Compressive stress/strain curves.

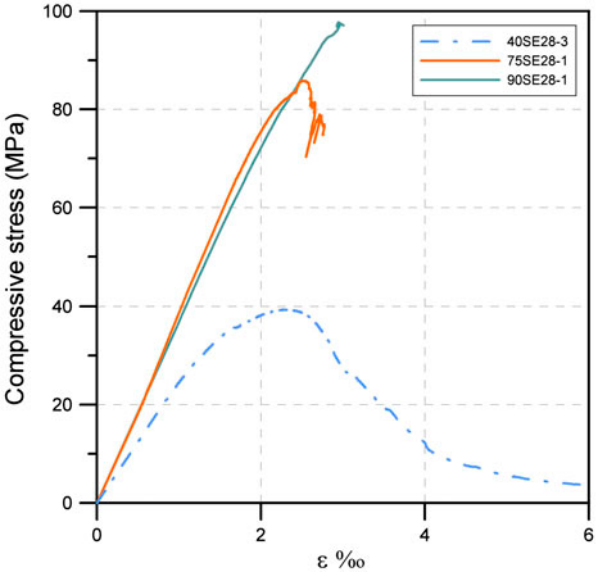

Figure 4. Comparison of compressive stress/strain curves for the several mixes.

As it can be noticed the strain parameters for all the LSC mixes are slightly lower with respect to the relevant class of NVC while a clear trend cannot be identified for the modulus of elasticity. However, for any concrete class, the flexural tensile strength is significantly higher in LSC than in NVC. This difference is likely to be reflected in a different bond behaviour.

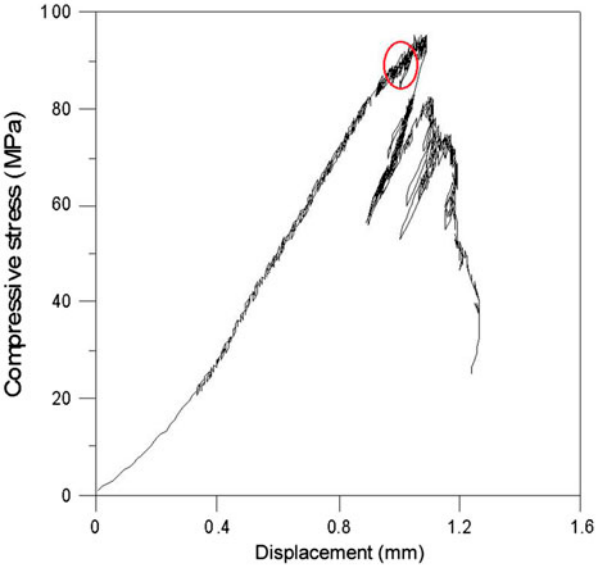

Figure 5. 90SE28-2 – Compressive stress/vertical displacement curve.

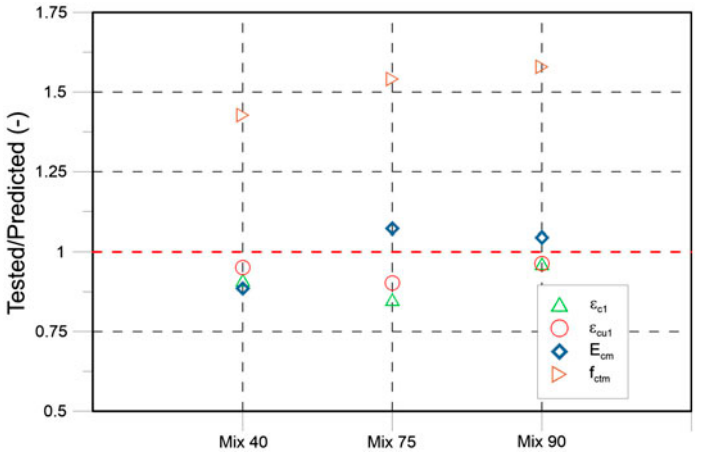

Figure 6. Properties at hardened state, ratio between experimental and predicted values.

3.2. Bond properties

Bond behaviour between concrete and reinforcement is a primary factor in designing reinforced concrete structures. It is well established that bond between a deformed bar and the concrete depends on several parameters, such as the concrete compressive and tensile strengths, the confinement due to the transverse reinforcement and the bar geometry (in terms of diameter and shape of the ribs).

Several researchers (Cattaneo & Rosati, 2009; Chan, Chen, & Liu, 2003; Collepardi, Borsoi, Collepardi, & Troli, 2005; Lorrain & Daoud, 2002; Valcuende & Parra, 2008; Zhu, Sonebi, & Bartos, 2004) investigated bond strength in SCC considering pull-out tests on a single bar according to CEB/RILEM test method or similar ones, or considering different shapes of specimens (i.e. walls) to assess the so-called "top bar effect". Considering the first type of test, the scatter of the experimental results is relevant (Collepardi et al., 2005; Domone, 2007), with differences between the bond strength of steel to NVC and of steel to SCC ranging between 0 and 70% (Collepardi et al., 2005).

Nevertheless, some authors (Collepardi et al., 2005; Zhu et al., 2004) studied the microstructure of the cement matrix and the Interfacial Transition Zone (ITZ) and they concluded that the increased bond strength in SCC is due to a more uniform ITZ and to more homogeneous distribution of fine voids. Because of the great differences in the properties of NVC and SCC, bond performance is expected to be different in the two cases.

Several studies have been carried out to evaluate the bond performance of SCC (see for instance, Sonebi & Bartos, 2002; Zhu & Bartos, 2003). The results of these studies suggest that SCC may exhibit significantly larger values of bond strength with respect to ordinary concrete. However, some contradictory results can be found regarding "size effect" in SCC; some authors even found that the bond strength increases with the bar diameter (Lorrain & Daoud, 2002).

For these reasons, an experimental investigation on the bond performance of ribbed bars set in Mixes 40, 75 and 90 has been carried out. For each mix, three groups of cylindrical specimens with three different bar diameters, 8, 16 and 24 mm, were tested to evaluate the average bond stress–displacement curves (nine specimens for each mix). The results are compared with previous research on similar specimens made of NVC and SCC.

3.2.1. *Experimental research*

For each mix, three groups of cylindrical specimens with an embedded ribbed steel bar (B450C) were tested. With constant cover/bar diameter ratio and height/bar diameter ratio, three different bar diameters were considered (ϕ8, ϕ16, ϕ24 – see Figures 7 and 8).

In order to prevent friction between the specimen and the support and to have three ribs embedded into the concrete, the effective bonded length was chosen equal to 2ϕ. Three specimens for each size were tested.

The testing system consisted of a closed-loop electromechanical Instron load frame with a maximum capacity of 100 kN. A specific device was added to the load frame to connect the testing machine to the specimen (Figure 9). The specimens were set inside a steel cylinder connected to the fixed cross-piece and to the actuator. The bottom of the cylinder and of the frame slab had a hole that allowed the bar of the specimen to be clamped to the actuator. An LVTD was used to measure the slip of the bar (unloaded end). The circumferential elongation of an aluminium ring placed on the bottom of the specimen was recorded by a clip gauge and used as feedback signal of the servo-controller.

3.2.2. *Experimental results and discussion*

Attention was focused on the effects of the bar diameter on the bond strength and on the modes of failure. Splitting failure has always been observed. The bond stress is evaluated assuming a uniform stress distribution along the effective length of the bar. The average bond strength and the CoV are reported in Table 6. From previous experience (Cattaneo & Rosati, 2009), the selected values of concrete cover to bar diameter ratio was found to be suitable to detect the splitting to pull-out transition. However, due to the very dense matrix of the investigated mixes, the concrete cover is found to be inadequate to prevent splitting failure.

The experimental evidence shows that SCC exhibits higher bond strength with respect to the values expected for an ordinary concrete. It can be observed that there are significant differences in terms of strength among the three mixes, with a clear "size effect" for the Mix 40, a not well-defined size dependence for the Mix 75 and, apparently, an increase in nominal strength with respect to the size for Mix 90, as shown in Figure 10.

Figure 11 reports some selected bond stress/slip curves for Mixes 40 and 75. Even though splitting has been observed in all the cases, it can be seen that increasing the bar diameter leads to an increase in both the secant stiffness at failure and the brittleness.

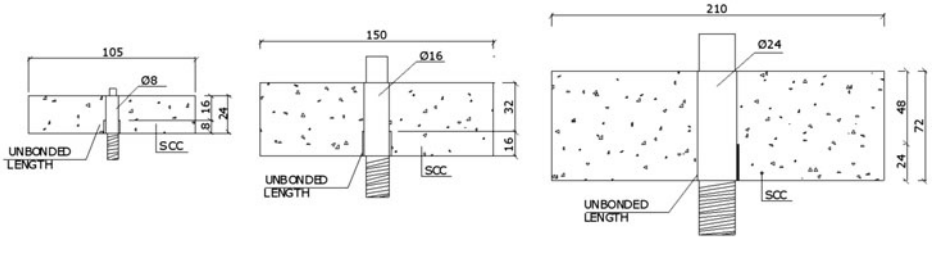

Figure 7. Geometry of specimens.

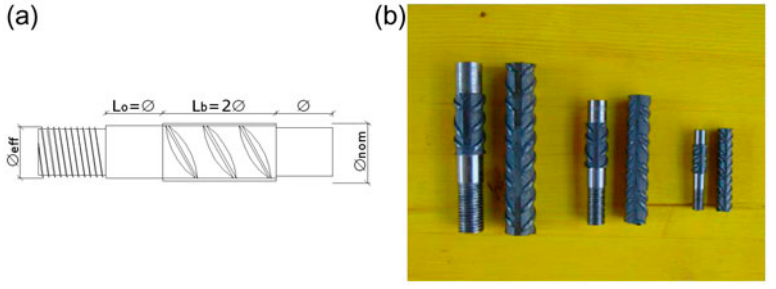

Figure 8. Geometry of bars.

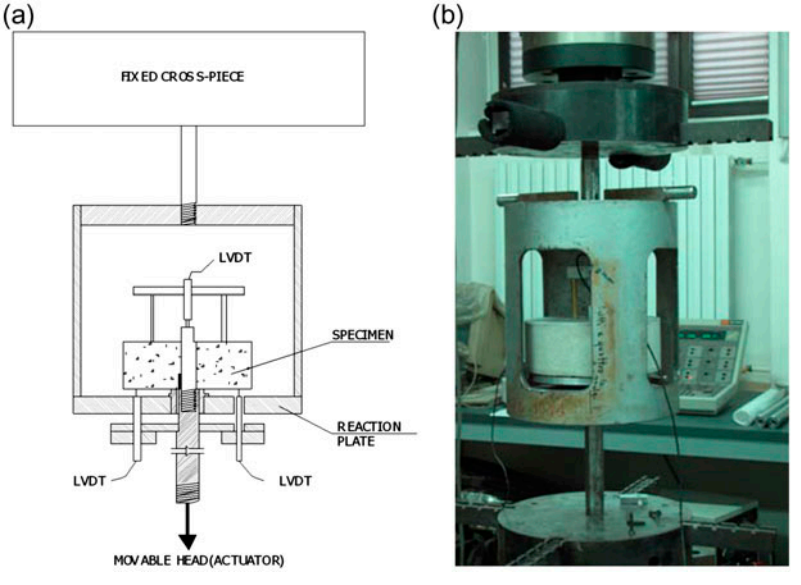

Figure 9. Testing device.

Table 6. Bond strength.

	$\phi 8$	$\phi 16$	$\phi 24$
Average C40/50 (MPa)	25.7	23.1	19.8
Average C75/90 (MPa)	28.2	37.1	27.4
Average C90/105 (MPa)	34.3	33.5	36.4
CoV C45/55 (%)	3.8	13.8	8.19
CoV C75/90 (%)	10.3	2.9	18.8
CoV C90/105 (%)	13.3	13.1	7.7

Additionally, it can be noticed that only in the case of Mix 40 it was possible to follow the descending branch. A higher compressive strength is always associated to a higher brittleness.

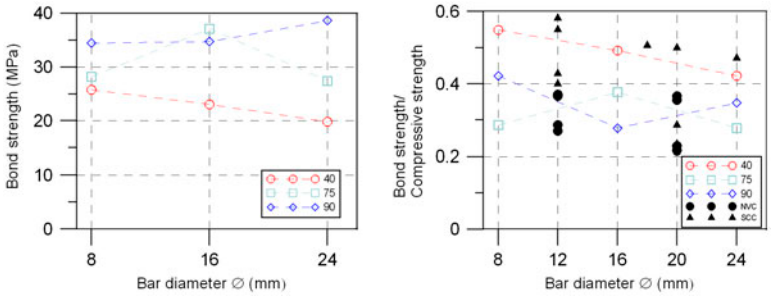

Figure 10. Bond strength vs. bar diameter (left) and bond/compressive strength ratio vs. bar diameter.

Figure 10 also shows experimental results compared to other tests on NVC and on SCC (Lorrain & Daoud, 2002; Sonebi & Bartos, 2002; Zhu & Bartos, 2002) in terms of ratio between the bond strength and the concrete compressive strength vs. bar diameter (see Table 7).

The experimental evidence shows very high bond strength with respect to the typical results obtained for NVC.

All the values for normal strength concrete are lower than .4. The obtained results on SCC show that the ratio between the bond strength and the compressive strength is in the range between .25 and .6. High strength LSC exhibits a lower bond strength/compressive strength ratio (between .28 and .39) with respect to normal strength SCC, which is almost in the same range than the ratio observed for ordinary concrete. When increasing the compressive strength, the increase in the bond strength is far from being proportional.

As previously mentioned, only Mix 40 shows a clear size dependence of strength on the bar diameter. The absence of size effect for Mixes 75 and 90 can be explained by the fact that these two mixes can be considered as high strength concrete and, in this type of concrete, the nominal strength seems to approach an asymptotic value for the

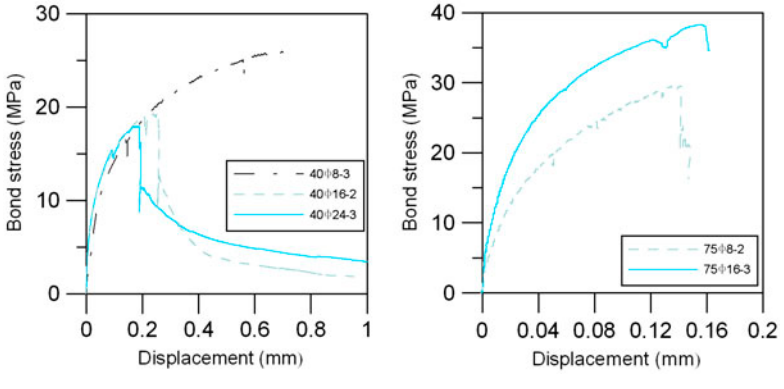

Figure 11. Bond strength vs. displacement (slip), Mixes 40 (left) and 75 (right).

considered concrete cover, which can be assumed in this case as the characteristic dimension (Cattaneo & Rosati, 2003).

A comparison between the experimental results and the prediction of the EC2 can be done. The average bond strength can be evaluated according to the following equation:

$$f_b = \frac{k}{\alpha_2} \times f_{ctm} \tag{2}$$

where k is a constant, assumed as equal to 2.25, according to EC2, Section 8.4.2; α_2 is a factor that accounts for the effect of large concrete cover, and it is evaluated according to EC2, Section 8.4.4; f_{ctm} is the average flexural tensile strength.

The value of f_{ctm} can be either provided by the EC2 for the relevant concrete class (NVC) or taken as equal to the experimental one (LSC-as reported in Table 4).

For both approaches, Figure 12 reports a comparison between the tested and the predicted values of the average bond strength. A value equal to one indicates that the same relationship between bond strength and flexural tensile strength valid for NVC also holds for LSC.

The first comparison (based on EC2 values of f_{ctm}) shows that, for any concrete class, the tested bond strength for LSC is more than the double than the predicted value for a NVC of the same class. These results could be expected since, as previously shown in Figure 6, the tested flexural tensile strength in LSC in approximately 50% higher respect to the predicted values for NVC for the same concrete class.

Additionally, even when adopting the experimental values, the second comparison shows that the relationship between bond strength and flexural tensile strength proposed by the EC2 is significantly conservative when applied to LSC.

Finally, as previously noticed, it has to be remarked that in no case splitting failure was prevented by the concrete cover. Since splitting forces are induced by the ribs of the deformed bars, it can be thus supposed that ribs of lower height may induce lower splitting forces. Consequently, Figure 13 compares, for LSC 90 and diameter $\phi = 16$ mm the load-slip behaviours of a specimen with an ordinary deformed bar and of a specimen

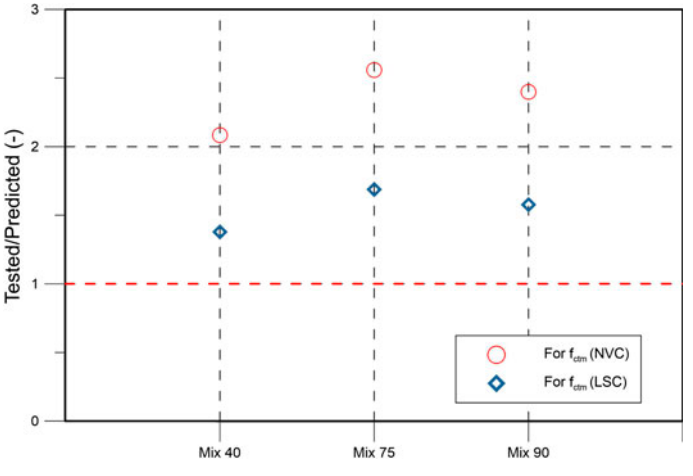

Figure 12. Bond strength, ratio of experimental to predicted value.

Table 7. Average values of bond strength/cylindrical compressive strength ratio.

Concrete class	$\phi 8$	$\phi 16$	$\phi 24$
C40/50	.55	.49	.42
C75/90	.29	.38	.28
C90/105	.33	.32	.35

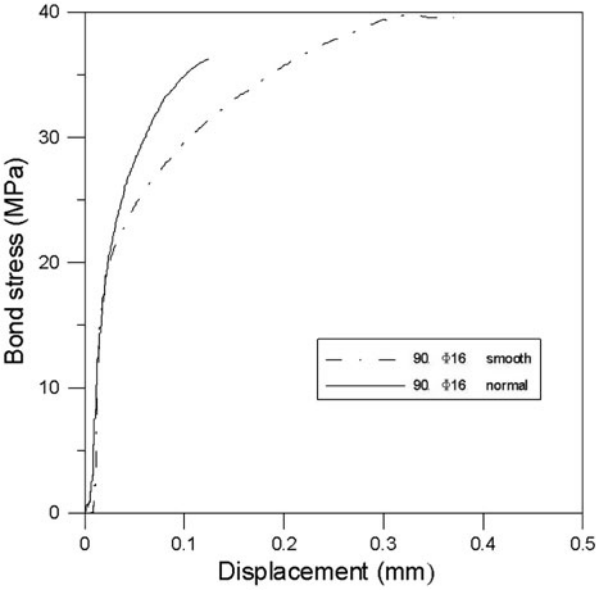

Figure 13. Bond strength vs. bar diameter for ordinary and smoothed bar.

where the ribs had been "smoothed" to one half of the original depth prior to casting. Splitting failure has still been observed, but the "smoothed" specimen definitively shows a more ductile behaviour and slightly higher bond strength. This suggests that when using LSC particular care has to be adopted to confine the effect of splitting forces.

4. Conclusions

Tests at the fresh state pointed out that LSC 40 is generally more suitable for various types of structural elements. This versatility of the material can have a draw back when uncertainty in casting time is expected. On the contrary, LSC 75 and LSC 90 (both I and II) show some properties that remain constant during a larger time period. Nonetheless, the high viscosity of the material (in particular mixes 90) suggests a very careful evaluation of the job-site conditions.

However, for all of the mixes, the use on job-site must be preceded by an accurate experimental investigation taking into account also of the effective mixing procedure (plant or agitator truck).

At hardened state the mixes LSC 40, LSC 75 and LSC 90 can actually be classified according to EC2 as C40/50, C75/90 and C90/105, respectively, and they can be designed according to the design rule of EC2, with some differences with respect to the bond properties.

Regarding bond behaviour, it is found that LSC exhibits higher bond strength and a more brittle behaviour with respect to NVC, in agreement with the results found in literature for SCC. The dependence of the bond strength on the dimensions of the rebar cannot be clearly established.

References

Cattaneo, S., & Mola, F. (2012). Assessing the quality control of self consolidating concrete properties. *Journal of Construction Engineering and Management, 138*, 197–205.

Cattaneo, S., & Rosati, G. (2003). Strength and size effect in fiber-reinforced materials. In N. Banthia, M. Criswell, P. Tatnall, & K. Folliard (Eds.), *ACI-SP216: Innovations in fiber-reinforced concrete for value* (pp. 63–78). Farmington Hills, MI: American Concrete Institute.

Cattaneo, S., & Rosati, G. (2009). Bond between steel and self-consolidating concrete: Experiments and modelling. *ACI Structural Journal, 106*, 540–550.

Chan, Y., Chen, Y., & Liu, Y. (2003). Development of bond strength of reinforcement steel in self-consolidating concrete. *ACI Structural Journal, 100*, 490–498.

Collepardi, M., Borsoi, A., Collepardi, S., & Troli, R. (2005). Strength, shrinkage and creep of scc and flowing concrete. In *Proceedings of SCC 2005 Conference on Center for Advanced Cement Based Materials* (pp. 911–920). Northwestern University, USA.

Desnerck, P., De Schutter, G., & Taerwe, L. (2012). Stress-strain behaviour of self-compacting concretes containing limestone fillers. *Structural Concrete, 13*, 95–101.

Domone, P. (2007). A review of the hardened mechanical properties of self-compacting concrete. *Cement and Concrete Composites, 29*(1), 1–12.

EFNARC. (2005). *The European guidelines for self-compacting concrete specification, production and use*. Retrieved from www.efnarc.org

Eurocode 2. (2004). *Eurocode 2: Design of concrete structures EN 1992*. Brussels, Belgium: European Committee for Standardization.

Klug, Y., & Holschemacher, K. (2003). Comparison of the hardened properties of self compacting and normal vibrated concrete. In *Proceedings of the 3rd International Rilem Symposium on Self Compacting Concrete*, Reykjavik, Iceland (pp. 596–605). Budapest.

Lorrain, M., & Daoud, A. (2002). Bond in self-compacting concrete. In *Proceedings of RILEM International Symposium Bond in Concrete from Research to Standards* (pp. 529–536). Budapest.

Sonebi, M., & Bartos, P. (2002). Bond behavior and pull-out test of self compacting concrete. In *Proceedings of RILEM International Symposium on Bond in Concrete from Research to Standards* (pp. 511–519). Budapest.

UNI 11040. (2003). *Calcestruzzo autocompattante – Specifiche, caratteristiche e controlli* [Self-compacting concrete- specification, properties and test methods]. Milano: UNI - Ente Italiano di Normazione.

UNI 6556. (1976). *Tests of concretes. Determination of static modulus of elasticity in compression*. Milano: UNI - Ente Italiano di Normazione.

UNI EN 12390-3. (2003). *Testing hardened concrete – Compressive strength of test specimens*. Milano: UNI - Ente Italiano di Normazione.

UNI EN 12390-5. (2003). *Testing hardened concrete – Flexural strength of test specimens*. Milano: UNI - Ente Italiano di Normazione.

UNI EN 12390-6. (2002). *Testing hardened concrete – Tensile splitting strength of test specimens*. Milano: UNI - Ente Italiano di Normazione.

Valcuende, M., & Parra, C. (2008). Bond behaviour of reinforcement in self-compacting concretes. *Construction and Building Materials, 23*, 162–170.

Zhu, W., & Bartos, P. J. M. (2002). Micromechanical proprieties of interfacial bond in self compactig concrete. In *Proceedings of RILEM International Symposium on Bond in Concrete from Research to Standards* (pp. 387–394). Budapest.

Zhu, W., & Bartos, P. J. M. (2003). Permeation properties of self-compacting concrete. *Cement and Concrete Research, 33*, 921–926.

Zhu, W., Sonebi, M., & Bartos, P. J. M. (2004). Bond and interfacial proprieties of reinforcement in self-compacting concrete. *Materials and Structures, 37*, 442–448.